Doppler Curves in Satellite Tracking and Characterization

Principal Author: David Richmond
Lockheed Martin
Co-Author: Katrina Raichle
Lockheed Martin

CONFERENCE PAPER

1. ABSTRACT SUMMARY

Our team evaluated the Doppler frequency shift of satellite signals observed by a user on the ground as a function of time. Expressions for determining the radial velocity and position of the satellite using the Doppler frequency shift are derived. Four orbital types are evaluated: LEO, MEO, GEO and Inclined GEO. Modification in our collection cadence and analysis approach for these orbital regimes with rationale is provided. Observed maneuver data collections are highlighted with computed changes in velocity and maneuver time. The benefits of such information are discussed, to include alternative catalog maintenance sensor, maneuver tip and queue, and anomaly resolution support.

2. INTRODUCTION

The ability to determine the current position and velocity and to predict the future position of satellites (metric data) has been a need ever since the first objects were launched into orbit. This initial Space Surveillance Network (SSN) comprised a network of phased array radar sensors, many of which had a primary mission other than tracking satellites. When satellites began to utilize geosynchronous orbits (GEO), optical telescopes were added to the SSN in order to augment the phased array space tracking capabilities. The methods used to identify the observed object rely heavily on the object's actual position with respect to the object's expected position. Errors in the expected position have caused misidentification, resulting in cross-tagging objects. Occasionally, objects may not be located at all because of maneuvers resulting in their placement on the lost list. These issues are more severe in the GEO regime due to the inability of ground based sensors to produced resolved images.

In recent years, the term "space surveillance" has been subsumed by the broader term "space situational awareness," which adds additional types of information to metric data with the goal of characterizing objects in space as well as the space environment itself. *Comparison of Phenomenology for Satellite Characterization* [1] identified satellite characteristics and mapped them phenomenology. Techniques of determining characteristics of on orbit objects was introduced in *Satellite Characterization Data Collection and Analysis* [2]. This mapping, shown in Figure 1, identified specific characteristics that can be obtained from each phenomenology. In this paper, our focus is the Radio Frequency (RF) signal produced by the satellite and the characteristics provided.

Attribute	Optical	Radar	IR	Signals
Metric-Position	Yes	Yes	Yes	Yes
Metric-Velocity	Yes	Yes	Yes	Yes
Physical - Size		Yes		
Physical - Mass		Support		
Physical - Bus	Yes	Support		
Orientation – rotation rate	Yes	Yes	Yes	
Orientation – axis of rotation	Yes	Yes	Yes	
Propulsion – Type	PoL	PoL	PoL	
Propulsion – Available Fuel	Support			
Propulsion – Delta Velocity	PoL	PoL	PoL	
Power – Production			Support	
Power - Consumption			Support	Support
Wireframe Diagram	Yes	Yes		
Material Composition	Yes			
Thermal Emissions			Yes	
Mission Status	Support	Support	Support	Yes
Gaseous Emissions			Yes	

Figure 1: Characterization Attributes

In order to collect signal information from an object of interest, an antenna is required. A typical antenna installation supports a specific operational system and is not available to be tasked for general passive collections. However, our research team in Valley Forge, PA obtained a decommissioned S-band Phased Array antenna that was still in operable condition. The antenna is currently being installed at our research site in Valley Forge for the purpose of conducting passive data collects of S-band signals from LEO, MEO and GEO regimes.

The Phased Array antenna provides a 60-degree field of view in the east-west direction as depicted in Figure 2. It consists of two 9'x8' panels, each providing 3 beams with 8 dB/K of gain. Alternatively, each panel can provide 6 beams with 5 dB/K of gain by leveraging a Phased Array antenna technique known as "beam partitioning." The electronically-steered array is capable of monitoring position and velocity of target objects, rapidly identifying when a maneuver has been performed by detecting gain fluctuations, geo-locating ground transmitters, and identifying electro-magnetic interference (EMI).

Phased Array Antenna

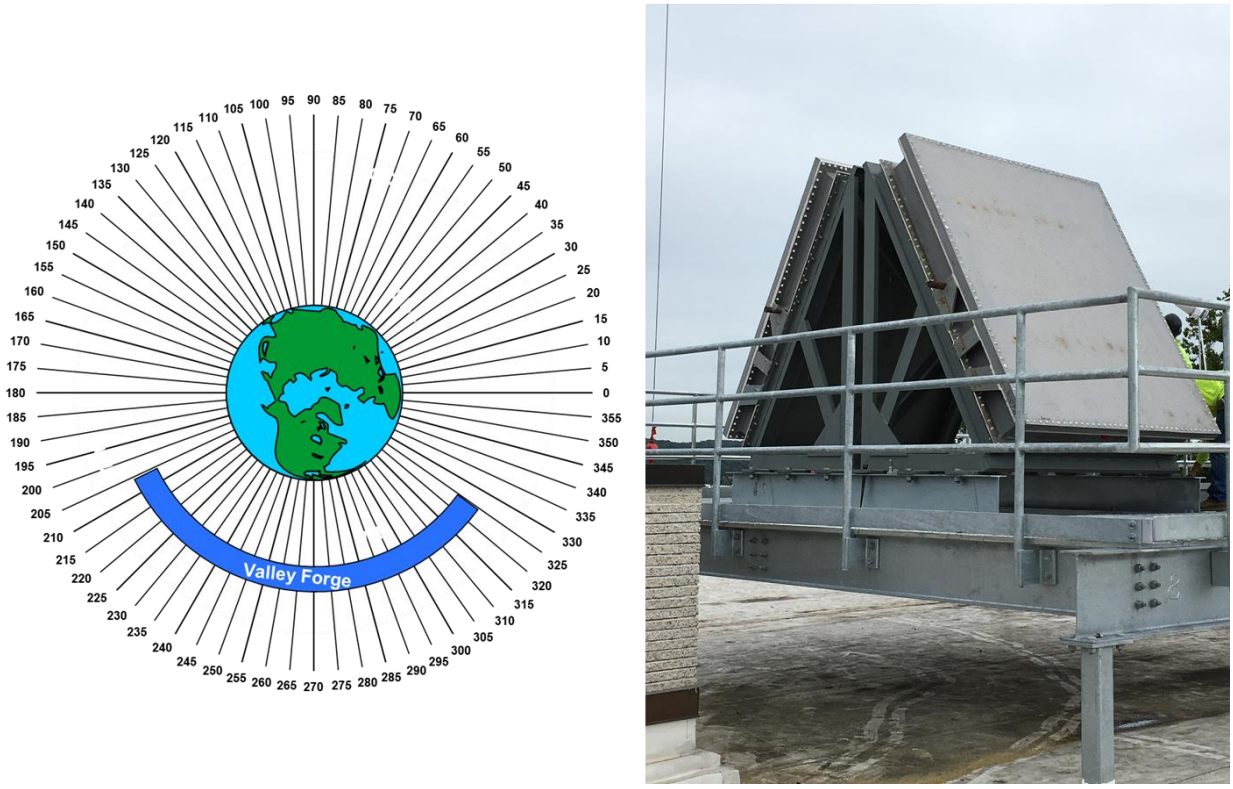

Figure 2: Phased Array Antenna

3. DOPPLER TRACKING

Observation of the Doppler frequency shift during a satellite pass can also provide sufficient information for accurate orbit determination. Velocity determination has been seen using Doppler shift measurements through a closed-form ECEF satellite acceleration formula derived from the rotation matrix method [3].

LEO's have been used in finding orbit and Doppler calculations that are used to derive general orbital models [4]. Doppler-aided velocity and position algorithms have been determined, but not to the point where they are used to form more actuate orbital determinations while actively tracking [5].

During the transit of a satellite in low earth orbit, the received signal frequency will typically vary from several thousand Hz above, to several thousand Hz below the transmitter frequency. Figure 3 shows a representative variation of frequency with time for a high inclination orbit, where the center frequency is 2245.673 MHz.

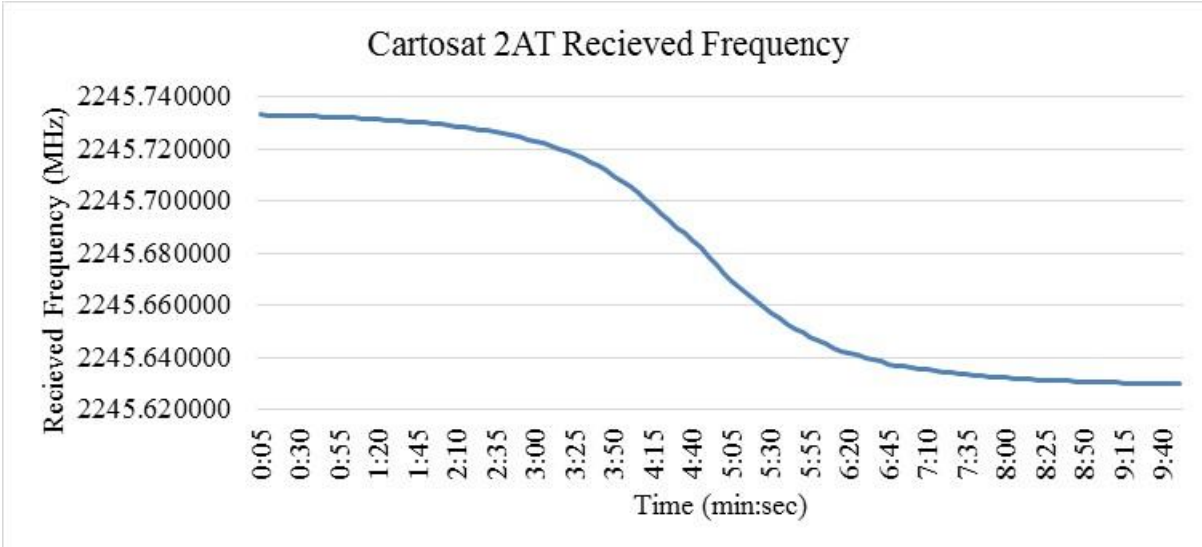

Figure 3: Graph of the received frequencies during an overhead pass of the Cartosat 2AT satellite from a location in Valley Forge, PA on the 6th of April 2018

4. COMPUTATION ALGORITHUM

The Doppler curve is a function of the relative motion between the receiving site and the satellite. Given the ground station coordinates are well determined, the only unknown components of the relative motion are due to the motion of the satellite, and the curve is solvable for the orbit. Conversely, if the satellite orbit is well determined, the location of the receiving station can be determined, and the satellite becomes useful for navigation.

The position of a satellite can be expressed as shift

$$r = R + \rho L \tag{1}$$

where R is the observation site position, ρ is the slant range, and L is a unit vector along the line of sight as shown in Figure 4. The position r may also be expressed in terms of an epochal position, r_0 and velocity v_0, where you have r_x, r_y, r_z and v_x, v_y, v_z [6].

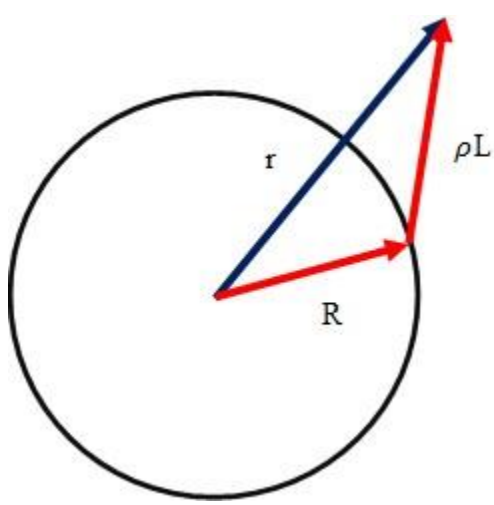

Figure 4: Satellite Position

Orbits may be directly fitted to the Doppler data in a trial and error fashion, but a much less laborious way of computing is to differentially correct an initial approximation of the orbit. The relative velocity between satellite and observer is computed from the Doppler shift

$$p = c\left(1 - \frac{f}{f_0}\right) \tag{2}$$

where f is the frequency received at the ground station and f_0 is the nominal transmitter frequency. p is defined as being positive when the relative separation is increasing. The Doppler shift is also proportional on the range rate,

$$p = \frac{f_0}{c}\dot{r} \tag{3}$$

where r is range, $\dot{r}$ is range rate, and c is the speed of light [4]. Relative velocity is a function of the geometry at some epoch, i.e., $p = f(r_0, v_0, R_0, V_0)$, where r_0 is the initial position of the satellite, v_0 is the initial velocity of the satellite, R_0 is the initial position of the ground antenna, and $V_0$is the initial velocity of the ground antenna. Below, both R_0 and V_0 are zero when taking measurements with reference from the ground antenna. Therefore, we have:

$$p = \frac{f_0[(r_x)(v_x) + (r_y)(v_y) + (r_z)(v_z)]}{c({r_x}^2 + {r_y}^2 + {r_z}^2)^{1/2}} \tag{4}$$

Since measurement of frequency is one dimensional at least six observations of the Doppler shift are necessary for a complete determination, due to the six unknowns that need to be solved for, $r_x, r_y, r_z, v_x, v_y, v_z$. Due to uncertainties in the preliminary orbit or errors caused by atmospheric drag and other perturbations, observed frequency shifts will differ, somewhat, from those predicted. The differences are called residuals and are computed from the differential of p. The differential of p is expressed:

$$dp = \left(\frac{\partial p}{\partial r_{x0}}\right) dr_{x0} + \left(\frac{\partial p}{\partial r_{y0}}\right) dr_{y0} + \left(\frac{\partial p}{\partial r_{z0}}\right) dr_{z0} + \left(\frac{\partial p}{\partial v_{x0}}\right) dv_{x0} + \left(\frac{\partial p}{\partial v_{y0}}\right) dv_{y0} + \left(\frac{\partial p}{\partial v_{z0}}\right) dv_{z0} + \left(\frac{\partial p}{\partial R_{x0}}\right) dR_{x0} + \left(\frac{\partial p}{\partial R_{y0}}\right) dR_{y0} + \left(\frac{\partial p}{\partial R_{z0}}\right) dR_{z0} + \left(\frac{\partial p}{\partial V_{x0}}\right) dV_{x0} + \left(\frac{\partial p}{\partial V_{y0}}\right) dV_{y0} + \left(\frac{\partial p}{\partial V_{z0}}\right) dV_{z0} \tag{5}$$

If all differentials are small, Equation (5) may be rewritten

$$\Delta p = \left(\frac{\partial p}{\partial r_{x0}}\right) \Delta r_{x0} + \left(\frac{\partial p}{\partial r_{y0}}\right) \Delta r_{y0} + \left(\frac{\partial p}{\partial r_{z0}}\right) \Delta r_{z0} + \left(\frac{\partial p}{\partial v_{x0}}\right) \Delta v_{x0} + \left(\frac{\partial p}{\partial v_{y0}}\right) \Delta v_{y0} + \left(\frac{\partial p}{\partial v_{z0}}\right) \Delta v_{z0} + \left(\frac{\partial p}{\partial R_{x0}}\right) \Delta R_{x0} + \left(\frac{\partial p}{\partial R_{y0}}\right) \Delta R_{y0} + \left(\frac{\partial p}{\partial R_{z0}}\right) \Delta R_{z0} + \left(\frac{\partial p}{\partial V_{x0}}\right) \Delta V_{x0} + \left(\frac{\partial p}{\partial V_{y0}}\right) \Delta V_{y0} + \left(\frac{\partial p}{\partial V_{z0}}\right) \Delta V_{z0} \tag{6}$$

Δp represents the residual of observed and computed relative velocities: Δr, Δv, ΔR, ΔV. The location of the antenna station is known, the corrections for ΔR and ΔV are zero. These terms become zero, leaving the residuals dependent only on the uncertainties in the orbit parameters.

The phased array antenna located in Valley Forge, PA was used to receive the signals. The Earth Centered Fixed (ECF) coordinates for this antenna is (1231.648, -4728.537, 4085.677). The satellite position and velocity values are computed relative to this position. For n observations we obtain the system of equations (7) where the partials are defined in equations (8) and (9).

$$\begin{bmatrix}\Delta p_1\\ \Delta p_2\\ \Delta p_3\\ \Delta p_4\\ \Delta p_5\\ \Delta p_6\end{bmatrix} = \begin{bmatrix} \frac{\partial p_1}{\partial r_{x0}} & \frac{\partial p_1}{\partial r_{y0}} & \frac{\partial p_1}{\partial r_{z0}} & \frac{\partial p_1}{\partial v_{x0}} & \frac{\partial p_1}{\partial v_{y0}} & \frac{\partial p_1}{\partial v_{z0}} \\ \frac{\partial p_2}{\partial r_{x0}} & \frac{\partial p_2}{\partial r_{y0}} & \frac{\partial p_2}{\partial r_{z0}} & \frac{\partial p_2}{\partial v_{x0}} & \frac{\partial p_2}{\partial v_{y0}} & \frac{\partial p_2}{\partial v_{z0}} \\ \frac{\partial p_3}{\partial r_{x0}} & \frac{\partial p_3}{\partial r_{y0}} & \frac{\partial p_3}{\partial r_{z0}} & \frac{\partial p_3}{\partial v_{x0}} & \frac{\partial p_3}{\partial v_{y0}} & \frac{\partial p_3}{\partial v_{z0}} \\ \frac{\partial p_4}{\partial r_{x0}} & \frac{\partial p_4}{\partial r_{y0}} & \frac{\partial p_4}{\partial r_{z0}} & \frac{\partial p_4}{\partial v_{x0}} & \frac{\partial p_4}{\partial v_{y0}} & \frac{\partial p_4}{\partial v_{z0}} \\ \frac{\partial p_5}{\partial r_{x0}} & \frac{\partial p_5}{\partial r_{y0}} & \frac{\partial p_5}{\partial r_{z0}} & \frac{\partial p_5}{\partial v_{x0}} & \frac{\partial p_5}{\partial v_{y0}} & \frac{\partial p_5}{\partial v_{z0}} \\ \frac{\partial p_6}{\partial r_{x0}} & \frac{\partial p_6}{\partial r_{y0}} & \frac{\partial p_6}{\partial r_{z0}} & \frac{\partial p_6}{\partial v_{x0}} & \frac{\partial p_6}{\partial v_{y0}} & \frac{\partial p_6}{\partial v_{z0}} \end{bmatrix} \cdot \begin{bmatrix}\Delta r_{x0}\\ \Delta r_{y0}\\ \Delta r_{z0}\\ \Delta v_{x0}\\ \Delta v_{y0}\\ \Delta v_{z0}\end{bmatrix} \tag{7}$$

$$\frac{\partial p}{\partial r_x} = \frac{f_0}{c}\left[\frac{v_x\left({r_x}^2 + {r_y}^2 + {r_z}^2\right) - r_x(r_x v_x + r_y v_y + r_z v_z)}{({r_x}^2 + {r_y}^2 + {r_z}^2)^{3/2}}\right] \tag{8a}$$

$$\frac{\partial p}{\partial r_y} = \frac{f_0}{c}\left[\frac{v_y\left({r_x}^2 + {r_y}^2 + {r_z}^2\right) - r_y(r_x v_x + r_y v_y + r_z v_z)}{({r_x}^2 + {r_y}^2 + {r_z}^2)^{3/2}}\right] \tag{8b}$$

$$\frac{\partial p}{\partial r_z} = \frac{f_0}{c}\left[\frac{v_z\left({r_x}^2 + {r_y}^2 + {r_z}^2\right) - r_z(r_x v_x + r_y v_y + r_z v_z)}{({r_x}^2 + {r_y}^2 + {r_z}^2)^{3/2}}\right] \tag{8c}$$

$$\frac{\partial p}{\partial v_x} = \frac{f_0}{c}\left[\frac{r_x}{\left({r_x}^2 + {r_y}^2 + {r_z}^2\right)^{\frac{1}{2}}}\right] \tag{9a}$$

$$\frac{\partial p}{\partial v_y} = \frac{f_0}{c}\left[\frac{r_y}{\left({r_x}^2 + {r_y}^2 + {r_z}^2\right)^{\frac{1}{2}}}\right] \tag{9b}$$

$$\frac{\partial p}{\partial v_z} = \frac{f_0}{c}\left[\frac{r_z}{\left({r_x}^2 + {r_y}^2 + {r_z}^2\right)^{\frac{1}{2}}}\right] \tag{9c}$$

To resolve the satellites position and velocity a minimum of six measurements is necessary to resolve the six unknowns. Increasing the number measurements provides increased precision in the results.

5. Results Summary

This approach was conducted on different orbital regimes to include Low Earth Orbits (LEO), Medium Earth Orbits (MEO, Geosynchronous Orbits (GEO) and Inclined GEO (IGEO) satellites.

LEO

Cartosat 2AT was the LEO satellite selected for the experiment. An initial estimate of the satellites orbit is necessary to point the antenna and track the satellite. This was obtained through previously developed pointing data software utilizing a Two-Line Element (TLE) set information as well as an accurate time source.
To understand the magnitude of the Doppler shift, it was necessary to determine the frequency in which the satellite was transmitting. This was done by recording the received frequency every 5 seconds for a single pass Figure 3. Next a graph of the derivative of the frequency over time was produced Figure 5. The maximum point on the derivative graph identified the frequency in which the spacecraft originally transmitted. This became the value used as the nominal frequency used to calculate the Doppler shift, p.

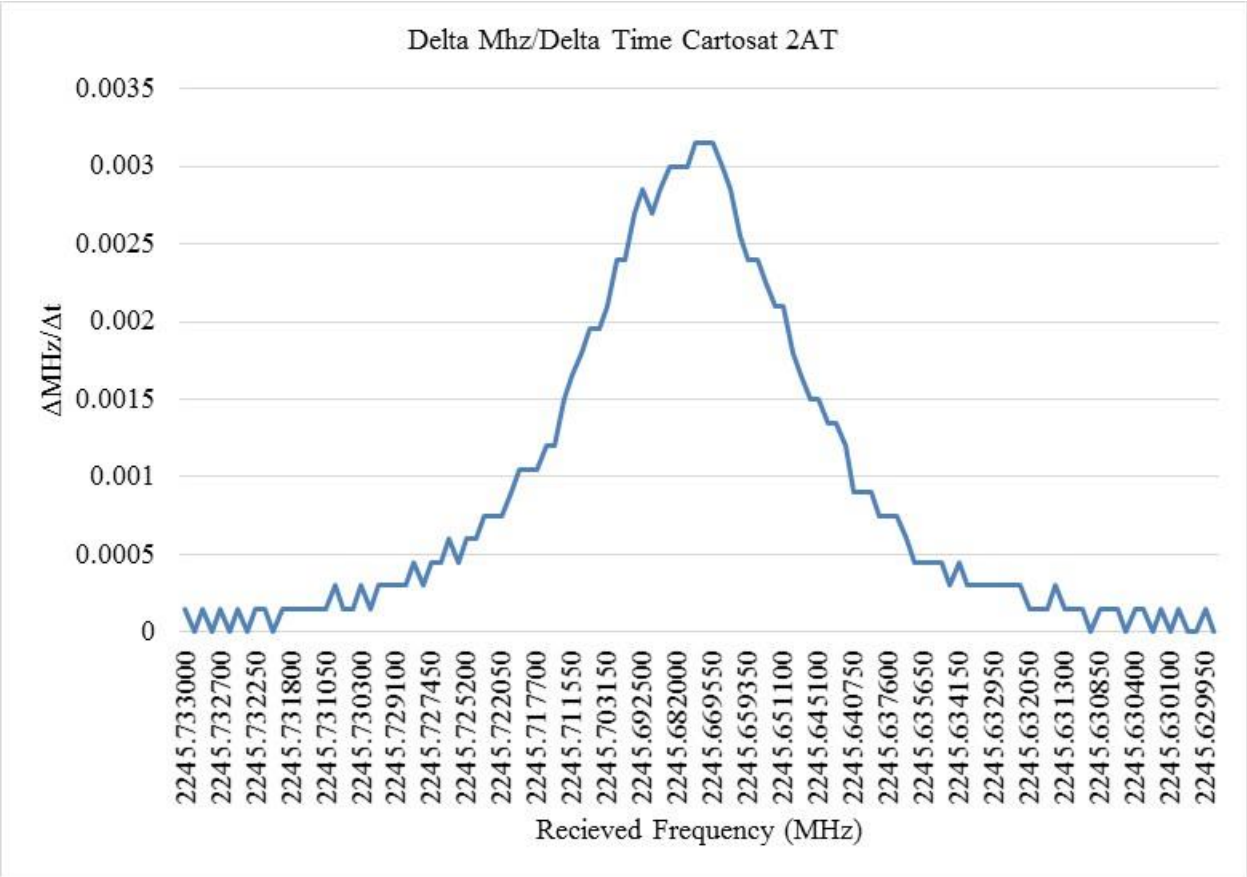

Figure 5: Derivative of frequency change over time for a pass of Cartosat 2AT on the 6th of April 2018.

Cartosat 2AT was recorded for a second time on the 8th of June and the derived equation 3 was tested to compare the predicted Doppler shift from the positional data and the actual Doppler shift. The results of this test are depicted in Figure 6.

A MATLAB simulation was done using equation 7 and therefore equations 8 and 9 performing a least squares calculation to determine if orbital estimations are more accurate when propagated 2 minutes into the future. We found that over extended propagations there was a decrease in residual angles between a predetermined truth position and velocity and our new orbit compared to the residual angle between the truth and the initial position and velocity. We are able to determine that we are creating a more accurate orbit determination.

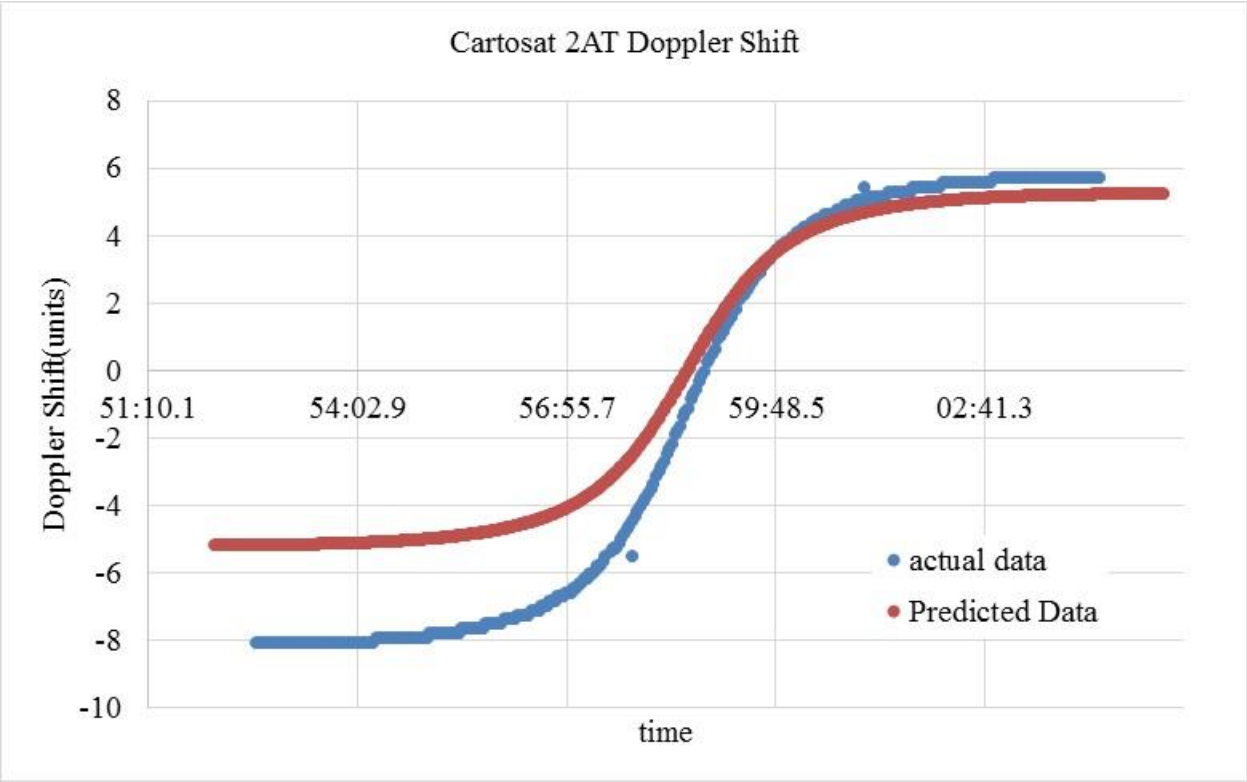

Figure 6: Measured and Predicted Doppler Shift found using the pointing data and equation 3 of Cartosat 2AT pass on the 8th of June 2018.

Better understand these differences between the actual and predicted results will become a topic for future research. Contributing factors include: ability to predict satellite position using TLE data, accuracy of data measurements (time and frequency), and residuals assumed as zero between equations 6 and 7.

MEO

A GPS was the MEO satellite selected for the experiment. A MEO satellite is in view of our ground received for several hours. However, a GPS satellite transmits for a small portion of the pass. On the 2nd March 2018 our team recorded received frequency over time for 45 minutes and produced a graph of this data shown in Figure 7. Each recorded data point is one minute apart. During this collection we observed 3 KHz movement in the received frequency. To understand the magnitude of the Doppler shift, it was necessary to determine the frequency in which the satellite was transmitting. Since we are unable to collect data over the entire pass, the LEO approach used to determine nominal frequency was unavailable. Our team was provided the expected nominal frequency (2227.513 MHz) used to calculate the Doppler shift, p.

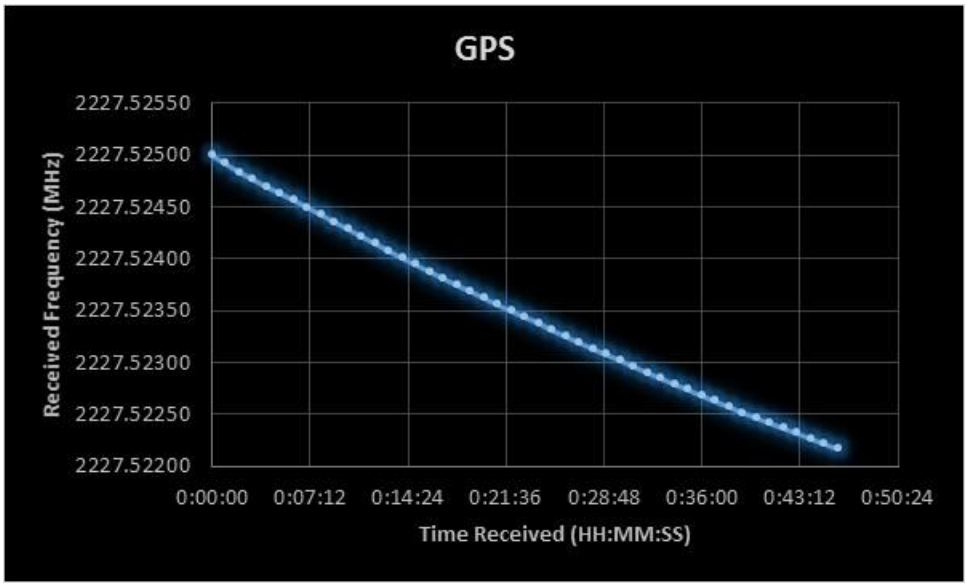

Figure 7: Received frequency from GPS satellite over Valley Forge, PA on 2nd March 2018

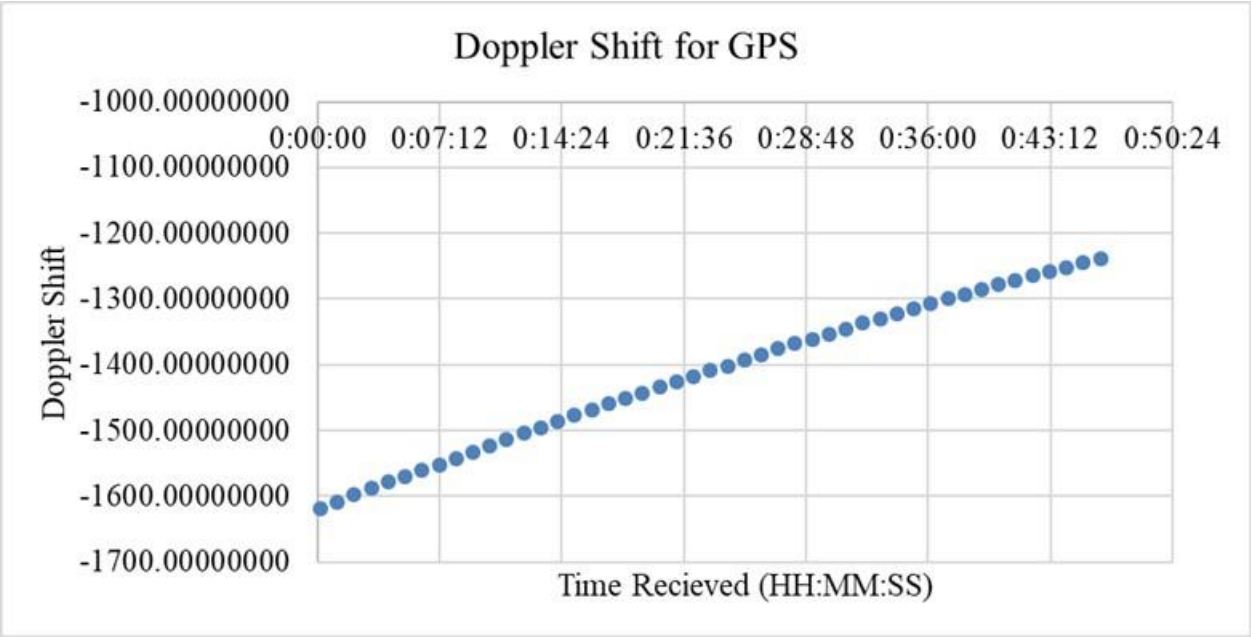

Figure 8: Doppler shift from GPS satellite over Valley Forge, PA on 2nd March 2018

Using the algorithm described above and the observed Doppler shift depicted in Figure 8, position and velocity information can be obtained. Although no maneuvers were observed during our experiments, rapid changes in velocity are detectable using this approach.

GEO

The GOES 17 was the GEO satellite selected for the experiment. This satellite was selected because it is maintained in a very tight box and has a very small Doppler shift. A new approach was necessary to determine the original transmitting frequency. Specifically, the vehicle was monitored continuously for 24 hours and the average received frequency was used, with the change measured in Hz. The received frequency over a 32 hour period was plotted against time (Figure 9) as well as the Doppler shift (Figure 10)

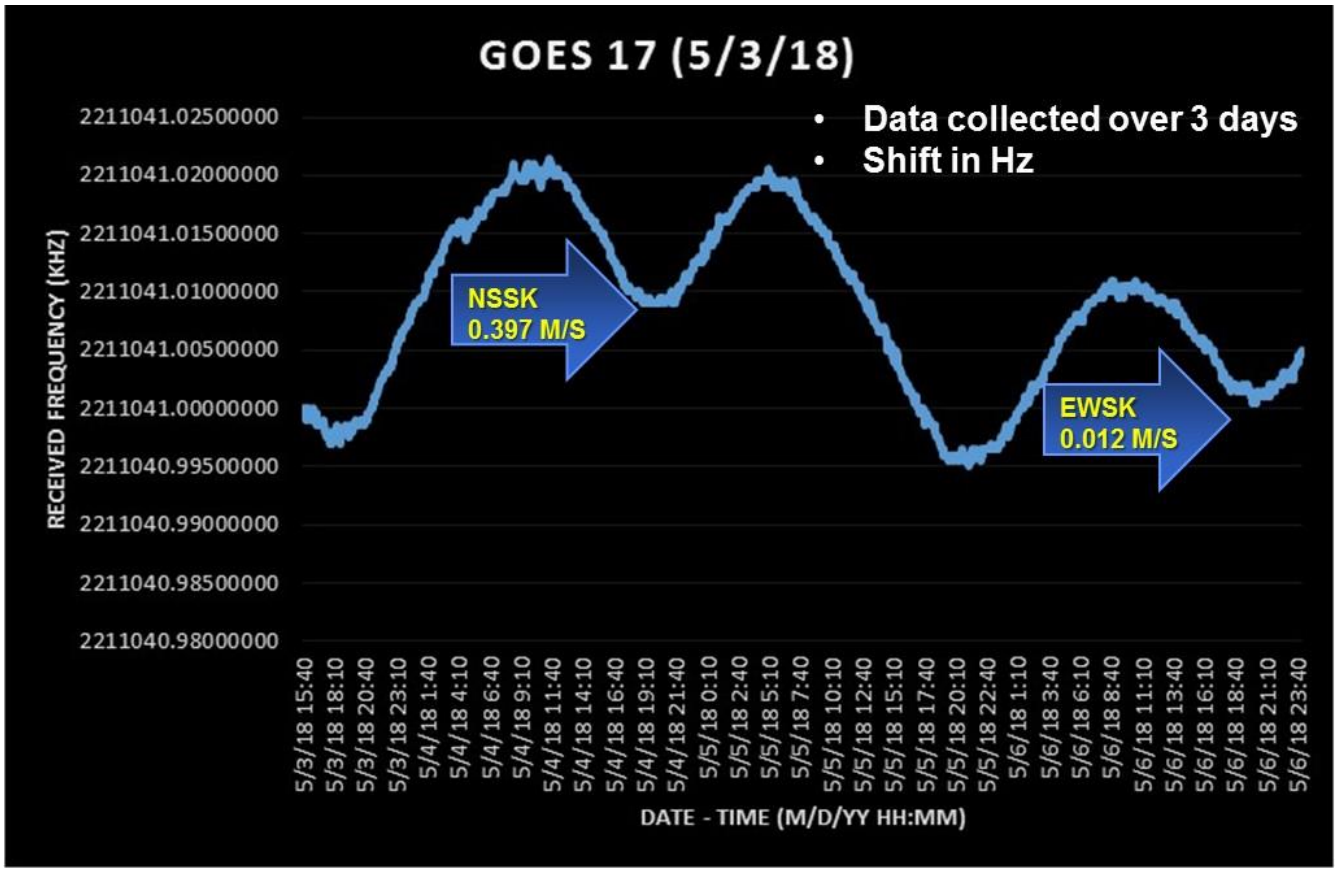

Figure 9: Received frequency from GOES 17 satellite over Valley Forge, PA starting on the 3rd of May 2018 going until the 6th of May 2018

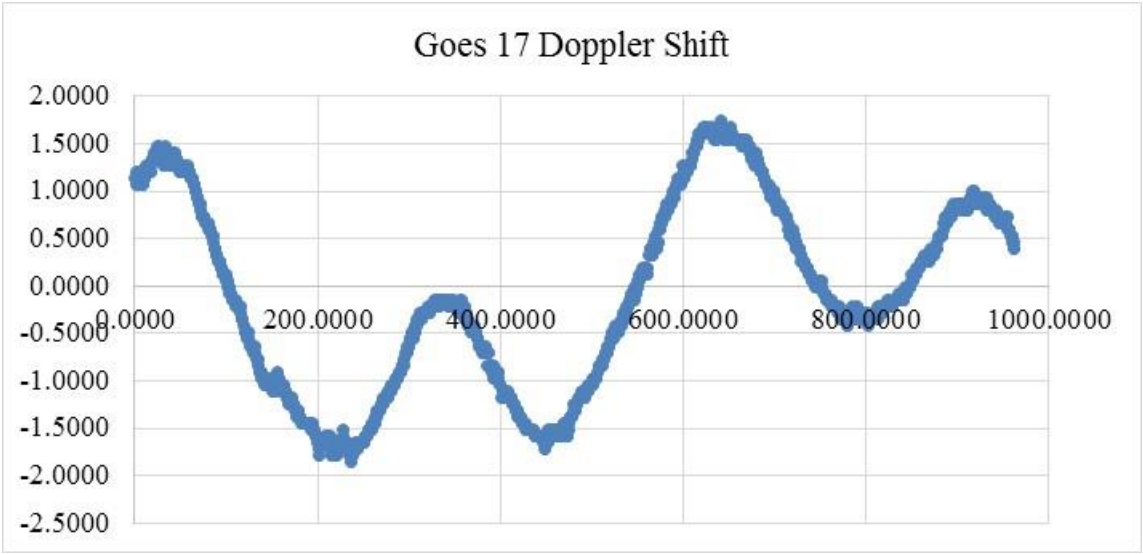

Figure 10: Doppler shift from GOES 17 satellite over Valley Forge, PA starting on the 3rd of May 2018 going until the 6th of May 2018

The received frequency was expected to be a sin curve, however deviations from this are believed to be maneuvers from the host. There was a known maneuver on May 4th, 2018 at 20:00. We discussed our results with the GOES

ground operators and they provided the maneuver history. This allowed our team to match the inflection points to maneuvers performed as shown in the figure above.

IGEO

Our team attempted an Inclined GEO collection on 14 May 2018. The receive frequency shifted at a rate greater than expected. Over an eight hour period the frequency moved 5 KHz and proceed out of our capture range. The ability to identify position, velocity and detect maneuvers for IGEO satellites is very similar to the GEO set. Therefore, no IGEO attempts have been completed since that date.

6. CONCLUSION

We are in the early stages of our research. We have established a set of desired satellite attributes that can be derived using an antenna that passively receives signals transmitted from on orbit objects. Our current effort verified position and velocity can be determined for multiple orbital regimes. Additionally, maneuvers can be identified as unexpected changes in the velocity. Our goal going forward is to evaluate approaches to improve the accuracy of the measurements and understand the residuals. Longer term we would establish a historical database for all objects to establish pattern of life baselines.

7. REFERENCES

1. Richmond, D., Spoto, G., *"Comparison of Phenomenology for Satellite Characterization"*, Proceeding of AMOS 2016 Technical Conference.
2. Richmond, D., and Brennan, J., *"Satellite Characterization Data Collection and Analysis"*, Proceeding of AMOS 2017 Technical Conference.
3. Zhang, J., Zhang, K., Grenfell, R., and Deakin, R., "*GPS Satellite Velocity and Acceleration Determination using the Broadcast Ephemeris*", The Journal of Navigation (2006), **59**, 293-305.
4. Zantou, E. B., Kherras, A., and Addaim, A., "*Orbit Calculation and Doppler Correction Algorithm in a LEO Satellite Small Ground Terminal*", Proceeding of 19th Annual AIAA/USU Conference on Small Satellites.
5. Simsky, A., and Boon, F., "*Carrier Phase & Doppler-Based Algorithms for Real-Time Standalone Positioning*", Septentrio NV, Belgium (2003).
6. Wright, J. R., *et al.*, "*Orbit Deamination Tool Kit*", Analytical Graphics Inc (2012).